Epilepsia, 50(4):605–616, 2009
doi: 10.1111/j.1528-1167.2008.01761.x

FULL-LENGTH ORIGINAL RESEARCH

Spatial localization and time-dependant changes of electrographic high frequency oscillations in human temporal lobe epilepsy

*Houman Khosravani, *Nikhil Mehrotra, *Michael Rigby, *Walter J. Hader, *C. Robert Pinnegar, *Neelan Pillay, *Samuel Wiebe, and *†Paolo Federico

*Hotchkiss Brain Institute and Department of Clinical Neurosciences, and †Department of Radiology, Faculty of Medicine, University of Calgary, Calgary, Alberta, Canada

Summary

Purpose: High frequency oscillations (HFOs) >200 Hz are believed to be associated with epileptic processes. The spatial distribution of HFOs and their evolution over time leading up to seizure onset is unknown. Also, recording HFOs through conventional intracranial electrodes is not well established. We therefore wished to determine whether HFOs could be recorded using commercially available depth macroelectrodes. We also examined the spatial distribution and temporal progression of HFOs during the transition to seizure activity.

Methods: Intracranial electroencephalography (EEG) recordings of 19 seizures were obtained from seven patients with temporal lobe epilepsy using commercial depth or subdural electrodes. EEG recordings were analyzed for frequency content in five spectral bands spanning DC-500 Hz. We examined the spatial distribution of the different spectral bands 5 s before and 5 s after seizure onset. Temporal changes in the spectral bands were studied in the 30-s period leading up to seizure onset.

Results: Three main observations were made. First, HFOs (100–500 Hz) can be recorded using commercial depth and subdural grid electrodes. Second, HFOs, but not <100 Hz oscillations, were localized to channels of ictal onset (100–200, 400–500 Hz, $p < 0.05$; 300–400 Hz, $p < 0.001$). Third, temporal analysis showed increased HFO power for approximately 8 s prior to electrographic onset ($p < 0.05$).

Conclusions: These results suggest that HFOs can be recorded by depth macroelectrodes. Also, HFOs are localized to the region of primary ictal onset and can exhibit increased power during the transition to seizure. Thus, HFOs likely represent important precursors to seizure initiation.

KEY WORDS: High frequency, Ripples, Fast ripples, Seizure localization, Temporal lobe epilepsy.

Electroencephalography (EEG) can measure functional brain activation as a manifestation of neuronal network activity. The range of frequencies recorded by EEG is typically limited to DC-100 Hz. This is due to the fact that most clinical centers use a sampling rate of 200 Hz (typically <500 Hz). With more widespread use of fast-sampling EEG machines (1–10 kHz), the relevant bandwidth of EEG has now expanded up to 600 Hz, where physiological activity in this range has been recorded in somatosensory cortex (Curio et al., 1994; Curio, 2000).

High frequency oscillations (HFOs; >80 Hz) can be classified by their ''operational'' frequency range and are commonly grouped into ripple (80–200 Hz) and fast ripple (FR; >200 Hz) frequency bands (Buzsaki et al., 1992). Ripples reflect network activity that includes both physiological and epileptiform activity (Rampp & Stefan, 2006). Specifically, ripples have been recorded in the hippocampus and entorhinal cortex in both normal (Buzsaki et al., 1992; Chrobak & Buzsaki, 1994) and epileptic neuronal networks (Buzsaki et al., 1992). Under nonepileptic conditions, ripples are believed to play a role in memory

Accepted June 11, 2008; Early View publication August 20, 2008.
Address correspondence to Paolo Federico, Departments of Clinical Neurosciences and Radiology, University of Calgary, Room C1241A, Foothills Medical Centre, 1403-29th Street N.W., Calgary, AB, T2N 2T9 Canada. E-mail: pfederic@ucalgary.ca

consolidation, transferring information from the hippocampus to the neocortex (Siapas & Wilson, 1998; Draguhn et al., 2000).

Ripples and FRs can cooccur under epileptic conditions. They have been observed exclusively at seizure foci in vitro (Dzhala & Staley, 2003; Lasztoczi et al., 2004; Khosravani et al., 2005) and in animal models of epilepsy (Bragin et al., 1999c, 2003). Ripples and FRs have also been observed in intracranial microelectrode EEG recordings from hippocampal and entorhinal cortices of epileptic patients (Bragin et al., 1999a, 1999b; Staba et al., 2002, 2004). FRs are seen predominantly at seizure foci in patients with temporal lobe epilepsy (Bragin et al., 2002a, 2002b; Staba et al., 2004; Ochi et al., 2007), and a positive correlation has been seen between the presence of FR and the presence of hippocampal atrophy and decreased neuronal density (Staba et al., 2007). Taken together, these findings suggest that pathological HFOs, and in particular FRs, serve as ''surrogate'' markers for the presence of an epileptic condition, and they may be important in generating some types of seizures (Traub et al., 2001, 2002; Bragin et al., 2004; Rampp & Stefan, 2006). For this reason, further study of HFOs is necessary to validate their role in this capacity.

Until recently, it was believed that HFOs could only be recorded using custom-built microdepth-electrodes. However, HFOs have recently been recorded using custom-built depth macroelectrodes (Jirsch et al., 2006; Urrestarazu et al., 2007) and commercially available subdural grid electrodes (Akiyama et al., 2005, 2006; Ochi et al., 2007). These studies also showed that HFO power amplitudes (FRs in particular) are typically the greatest at the primary ictal zone (Urrestarazu et al., 2007). Notably, previous studies of HFOs focused on interictal or ictal discharges, and few have studied discharges recorded during the preictal period.

The preictal state likely represents a critical state of brain activity prior to seizure initiation (Litt & Lehnertz, 2002; Federico et al., 2005). We have previously shown in an in vitro model of seizures that epileptiform discharges in the preictal period leading up to seizures show a specific and sharp increase in the HFO power (100–300 Hz) that does not occur at lower frequencies (0–100 Hz) (Khosravani et al., 2005). This suggests that HFOs may reflect underlying network activity that is specific to the interictal-to-ictal transition. However, very little is known about how spatial distribution of HFOs corresponds to temporal changes that may occur during the immediate pre-ictal epoch in humans. Indeed, if HFOs are true markers of epileptogenicity, they should localize to the ictal onset zone and should change during the transition into seizures. We therefore used spectral power analysis of intracranial EEG recordings of seizures in humans to test three hypotheses: (1) HFOs may be recorded with commercially available depth electrodes, (2) HFOs localize to specific contacts that correlate with the ictal onset zone, and (3) HFOs exhibit temporal changes during the transition to seizure.

Methods

Patient selection and EEG recordings

Informed consent was obtained from all patients involved in this study. Ethics approval was obtained from the University of Calgary Medical Bioethics Committee. We recruited seven consecutive patients with medically refractory epilepsy who underwent intracranial video EEG monitoring (VEM) from February to August 2006 as part of their presurgical workup at the University of Calgary Comprehensive Epilepsy Centre.

Each patient had commercially available subdural strip or grid platinum electrodes (2.3 mm contact, effective area 4.15 mm^2, 10 mm spacing, impedance <100 Ω) and depth electrodes (4–6 contacts, 2.3 mm width × 0.5 mm radius, effective area 7.2 mm^2, 10 mm spacing, impedance <100 Ω) implanted according to clinical need using standard protocols in our program (Ad-Tech Medical Instrument Corporation, Racine, WI, U.S.A.). Sites for electrode placement were selected based upon clinical history, as well as the following investigations: Previous scalp VEM, magnetic resonance imaging (MRI), single-photon emission computerized tomography, and neuropsychological assessment.

During admission for intracranial VEM, each patient's antiepileptic medications were reduced to increase the likelihood of recording seizures. EEG was acquired simultaneously on two EEG machines. The first machine (the clinical machine) sampled all implanted electrodes at a sampling rate of 500 Hz. The second machine (the research machine, SynAmp1; Compumedics Corp., El Paso, TX, U.S.A.) sampled a subset of electrode contacts (up to 13 due to a limited number of available connection inputs) at a sampling rate of 5 kHz, low-passed filtered at 1 kHz. The channels selected for recording by the research machine were identified by an electroencephalographer (P.F.) based on the expected seizure onset zone (presence of a structural lesion, previous scalp VEM data, etc.), and the interictal or ictal data were recorded by the clinical EEG machine during the first few days of intracranial VEM. In one patient (patient 3), the electrodes initially selected for sampling at 5 kHz were revised based the patient's subsequent pattern of seizure activity—only postrevision electrode sampling data were used in our analysis. Bipolar recordings were analyzed to avoid reference contamination and to more accurately localize HFOs, since they are believed to be locally generated phenomenon. Both machines recorded VEM data continuously, and the clinical EEG was read by the attending epileptologist. The clinical VEM data were used as a reference by an expert electroencephalographer (P.F.) to identify and clip subclinical and clinical

EEG events on the research machine. Seizure onset was determined by review of clinical EEG data in bipolar and referential montages and was identified as the time at which the background rhythm first changes (e.g., attenuation, rhythmic sharp waves, gamma activity, etc.). For each seizure, recordings were clipped for 30 min preceding electrographic seizure onset and 5 min after seizure onset (which is longer than the duration of all recorded seizures).

Time-frequency analysis

Continuous EEG was recorded at a sampling rate of 5 kHz (1 kHz low-pass Bessel filter) and analyzed using in-house software designed in Matlab (Mathworks Corp., Natick, MA, U.S.A.). Prior to analysis, all EEG signals were subjected to preprocessing involving removing linear trends (detrending) and removal of DC baseline shifts (Fig. 1A). The latter utilized a moving average filter, equivalent to a finite impulse response (FIR) high-pass filter ($f_c = 0.5$ Hz).

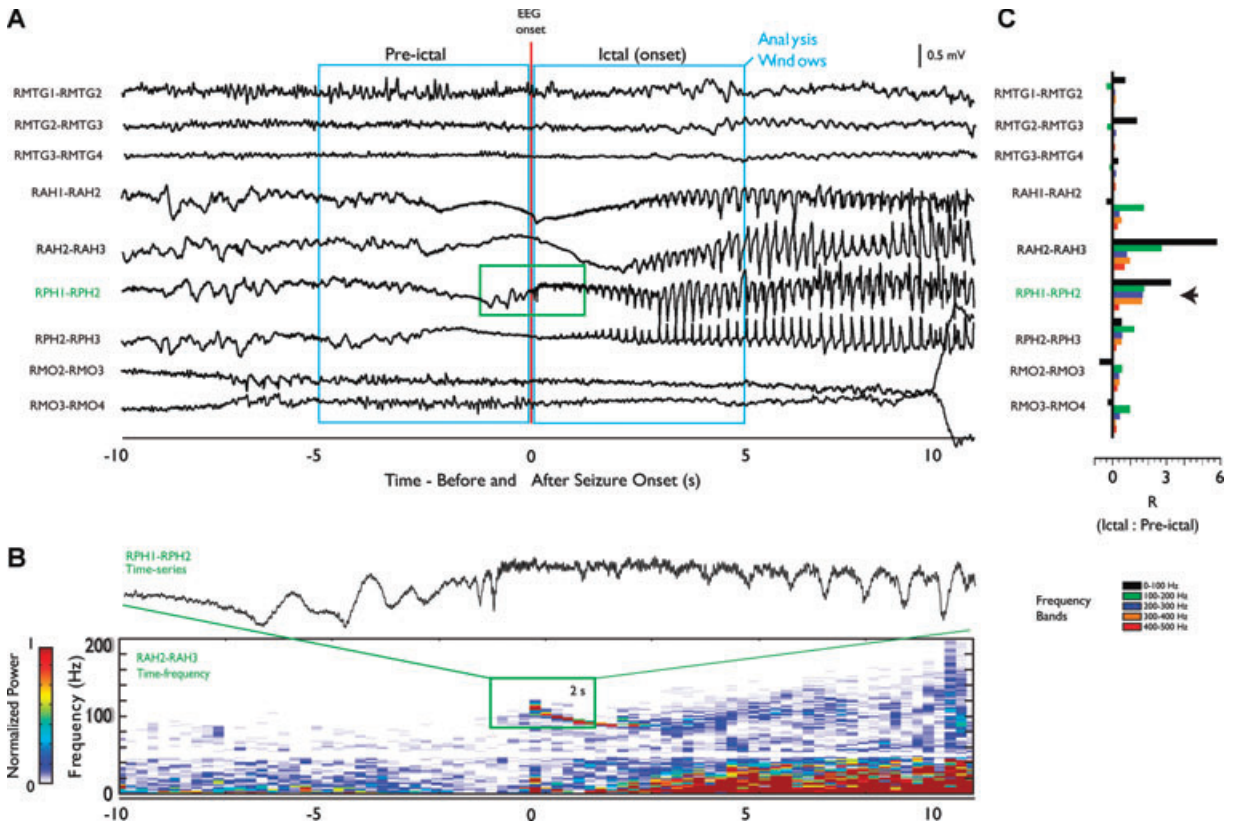

Figure 1.

HFOs can be recorded using commercially available strip electrodes and are recorded with maximal prevalence during the immediate preictal to ictal transition. (**A**) Intracranial EEG recording obtained at 5 kHz in the right amygdala, hippocampus, and occipital lobe in patient 6, who had a normal MRI and mild gliosis in the right amygdala and hippocampus on pathological examination (see Table 1). The channel label corresponding to electrographic onset is highlighted in green. (**B**) Time frequency representation for the primary ictal onset trace for the seizure shown in panel **A**. The appearance of HFOs, with a dominant frequency component at approximately 120 Hz is clearly visualized by increased power magnitude (bright red colors in highlighted in box). (**Inset**) The corresponding time series for 2 s of activity is visualized clearly showing HFOs; the corresponding region is also highlighted in panel **A** (green box). This increase lasts into the seizure but is most intense during the first 5 s, as slower spiking activity later predominates. Note that while the 0–200 Hz bands are shown in this figure, the power analysis was performed from 0–500 Hz in 100 Hz frequency bands (see Methods section). (**C**) Spatial (channel) distribution of periictal low frequency and HFO changes for each channel and each frequency band as compared for 5 s of power amplitude data between ictal and preictal analysis windows (see panel **A**); note maximal HFOs (100–500 Hz) in the channel of primary seizure onset. Arrow marks the channel of seizure onset.

Subsequently, each seizure recording (30 min preictal and 5 min ictal/postictal) was analyzed using a short-time Fourier transform (STFT) that provided a time-dependent measure of the signal's spectral composition in each channel (Fig. 1B). Continuous EEG data were passed to the STFT in ''running'' windows of 2-s segments with one-half overlap (effective temporal resolution of $\Delta t = 1$ s). These were analyzed by the STFT algorithm with a temporal resolution of 500 ms with one-half overlap windows, resulting in an effective frequency resolution of $\Delta f = 1$ Hz. The resulting three-dimensional data (consisting of time versus frequency versus power amplitude) was then summed in the frequency dimension into five frequency bands spanning 0–100 (low frequency), 100–200 (ripple), 200–300 (FR1), 300–400 (FR2), and 400–500 Hz (FR3). This procedure results in a time-dependent measure of spectral composition in five EEG bands. Equidistant bandwidths were selected in order to allow for meaningful statistical comparison across different bands. Note that the bulk of spectral power amplitudes exist in the 0–100 Hz band, as there is an inverse correlation between EEG frequency and spectral power. All individuals involved in data analysis were blinded to the location of seizure onset zones(s), and all other clinical data until all analyses were completed.

Spatial analysis of HFOs

In order to examine the relation between the presence of HFOs and regions (i.e., channels) of seizure onset, we compared two epochs of EEG for each channel—the immediate preictal and the first few seconds of seizure onset. This technique is similar to that introduced by Jirsch et al. (2006). Specifically, 5 s of power spectral amplitudes were summed preceding electrographic seizure onset (preictal) and compared with the first 5 s of seizure activity (Fig. 1A). A unitless ratio (relative power ratio, *R*) was then derived such that the seizure epoch (for each channel and each frequency band) was normalized to the preictal epoch as follows,

$$R(f',c) = \frac{\left(\sum_{f'=f}^{f+\Delta f}\sum_{t=0}^{5} P_c(t,f') - \sum_{f'=f}^{f+\Delta f}\sum_{t=-5}^{0} P_c(t,f')\right)\Delta t\Delta f}{\sum_{f'=f}^{f+\Delta f}\sum_{t=-5}^{0} P_c(t,f')\Delta t\Delta f} \qquad [Eq.1]$$

where t is time in seconds ($t = 0$ at electrographic onset), f' is the lower bound of frequencies in each band (in Hz, $f = \{0,100,200,300,400\}$), c is channel number ($c = \{1, \ldots, n\}$), and P is the power spectral amplitude (mV^2/Hz). The above calculation was performed for each band (frequency range $\Delta f = 100$ Hz) and each channel [resulting in $R_{(f,c)}$; see Fig. 1C]. Use of this normalized ratio was necessary to allow each patient and each seizure to act as their own control. This normalized ratio also allowed seizures across different patients to be compared. Note that positive *R*-values reflect an increase in HFO power during the ictal epoch, whereas negative values indicate a relative increase in HFO power in the immediate preictal period. We did not scale or normalize *R*-values from different bands in relation to a ''standard band'' (e.g., 0–100 Hz), since power amplitudes in each band may not be mutually exclusive as neuronal processes involved in generating seizures may have frequency components that span across different spectral bandwidths.

Statistical analyses were performed on the pooled results of seizures from each patient (i.e., intrapatient analysis). Seizures that originated from the same electrode(s) based on conventional review of the VEM data were grouped together, and their *R*-values were averaged and reported with SEM values. An analysis of variance (ANOVA) was then used to compare summed power amplitudes between frequency bands for each electrode.

Next, the mean power amplitude values for each frequency band were compared for three different channels: (1) The channel of electrographic seizure onset (i.e., origin), (2) the immediately adjacent channel, and (3) a distant noninvolved channel. An ANOVA was used with the Bonferroni correction to compute statistical significance for all permutations across bands (i.e., origin 0–100 Hz versus origin 100–200 Hz, etc.) and between the bands for different contact locations (origin 100–200 Hz versus distant 100–200 Hz, etc.).

Temporal analysis of HFOs

The change in power spectral amplitude for each band, for each channel, and over time during the immediate preictal epoch was evaluated. Once again, a similar unitless numerical quantifier was used to allow pooling of data across seizures and patients. The *R* quantity [$R_{(f,c)}(t)$] for this analysis was computed over time using a 5-s ''sliding'' analysis window that was compared to a fixed background epoch of equal duration (i.e., $\Delta t = 5$ s; see Fig. 2).

$$R(f,c,n)(t_i) = \frac{\left(\sum_{f'=f}^{f+\Delta f}\sum_{t=t_i}^{t_i+\Delta t} P_c(t,f') - \sum_{f'=f}^{f+\Delta f}\sum_{t=BKGND_n}^{BKGND_n+\Delta t} P_c(t,f)\right)\Delta t\Delta f}{\sum_{f'=f}^{f+\Delta f}\sum_{t=BKGND_n}^{BKGND_n+\Delta t} P_c(t,f)\Delta t\Delta f} \qquad [Eq.2]$$

$$\bar{R}_{(f,c)}(t_i) = \frac{\sum_{n=1}^{3} R(f,c,n)(t_i)}{3} \qquad [Eq.3]$$

Here i is the interval or analysis window number of Δt duration that was computed continuously for each channel leading up to electrographic seizure onset. Similar to the spatial analysis, $R_{(f,c,n)}(t)$ was computed for each band spanning the five frequency ranges (f' lower bound for

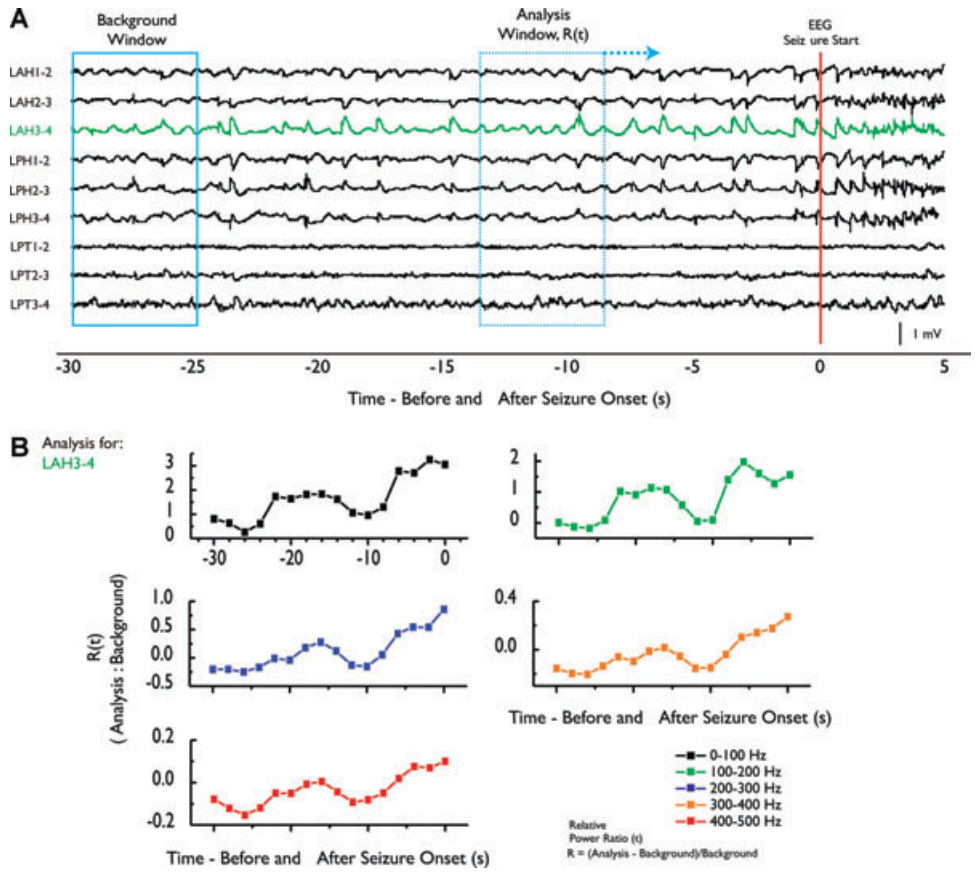

Figure 2.

Commercially available depth electrodes can be used to record HFOs, which undergo increases in power during the preictal period. (**A**) A 30-s segment of EEG sampled at 5 kHz leading to seizure onset recorded using commercially available depth macroelectrodes placed in the left hippocampus and amygdala in a patient with unilateral temporal epilepsy due to hippocampal sclerosis (Patient 1). Continuous (temporal) spectral power analysis was performed (see Methods section), and power amplitudes were summed in 5-s moving analysis windows for each channel and band. The continuous power amplitude data were compared to a background analysis window also of 5 s duration (see Methods section). This produced a time-dependent *R*-value [i.e., $R_{(f,c)}(t)$]. This process was performed for three independent background EEG windows and averaged. (**B**) Mean time-dependent relative power ratio (*R*-value) reported in a 2-s time resolution, in each band, for the channel of electrographic onset. Relative power increases can be seen at all frequencies during the period leading up to the onset of this seizure.

each band, $\Delta f = 100$ Hz) and also for each channel (c) separately. Three background EEG segments that showed no epileptiform activity were selected for each seizure by an electroencephalographer (P.F.; $n = 3$). Background segments were selected within the 30-min epoch, prior to but as close in time as possible to seizure onset. $R_{(f,c,n)}(t)$ was computed three separate times using each of the three background segments to minimize bias caused by background segment selection. Thus, the final time-dependent values for $R_{(f,c)}(t)$ were reported as a mean quantity (Equation 3; Fig. 2B). Note that Equation 2 does not show the additional step of overlapping analysis windows (one-half window overlap) as was described for the spatial analysis. Thus, the effective temporal resolution for $R_{(f,c,n)}(t)$ was 2.5 s. Subsequent statistical analysis and grouping of multiple seizures based on their site of origin was similar to that used for the spatial analysis.

Results

Patient characteristics

Seven patients (mean age 35 ± 7 years; four females) participated in the study, and a total of 19 seizures were recorded with continuous fast-sampling EEG (Table 1).

Table 1. Demographic, imaging, electrophysiological, pathological, and clinical characteristics of the study patients

Patient	Age/sex	MR Imaging	Electrode placement	Interictal discharge locations	Seizure onset	Pathology	Procedure/ outcome
1	30/M	Left ant temporal resection, residual left hippocampal sclerosis	Depth—LAH, LPH, LPT, LIO	Left ant and post hippocampus	[4] Left ant and post hippo	Hippocampal sclerosis	Left SAH/seizure-free
2	28/F	Right temporal horn slightly larger than left	1 × 8—LPF, RPF, RMF	Right amygdala and hippocampus	[1] Right amygdala and hippocampus	Hippocampal sclerosis	Right ATL/seizure-free
			1 × 4—LAM, LAH, RAM, RAH, RMTG				
3	44/F	Right middle temporal gyrus lesion, suspected DNET	8 × 8 grid—right TPFAP	Very frequent—right ant temporal, left amygdala, hippocampus	[3] Right ant and inf temporal gyrus	DNET	Lesionectomy and right SAH/seizure-free
			1 × 4 strip—RPH, RPT	Moderately frequent—right posttemporoparietal, right hippocampus	[2] Left amygdala		
			Depth—LAM, LAH				
4	28/M	Normal	Depth—LAM, LAH, LPH, RAM, RAH, RPH	Frequent—left ant and post-hippocampus	[2] Left ant hippocampus	Mild gliosis	Left SAH/seizure-free
				Less frequent—right ant and posthippocampus	[2] Right post- hippocampus		
5	36/F	Right hippocampal head atrophy, mild loss of internal architecture	Depth—LAM, LAH, LPH, RAM, RAH, RPH	Very frequent—right amygdala, right post hippocampus	[1] Right amygdala and ant hippocampus	Mild gliosis	Right SAH/seizure-free
				Moderately frequent—left amygdala, left post- hippocampus			
6	42/M	Normal	1 × 4 strip—RAM, RAH, RMTG, RMO, RSO	Right amygdala and hippocampus	[3] Right amygdala and hippocampus	Mild gliosis	Right SAH/seizure-free
7	41/F	Prior selective left SAH, with atrophy of remaining hippocampus and fornix	1 × 8 strip—LPF, RPF, RSTG	Frequent—left mid and ant temporal	[1] Left ant temporal	Mild gliosis	Left ATL/ongoing seizures
			1 × 4 strip—LAM, LAH, LMTG, RAH, RAM	Less frequent—left inf temporal	[1] Left frontal and Right ant tempo		

Square brackets in the fifth column denote the number of seizures recorded. ant, anterior; ATL, anterior temporal lobectomy; DNET, dysembryoplastic neuroepithelial tumor; F, female; inf, inferior; LAH, left anterior hippocampus; LAM, left amygdala; LPH, left posterior hippocampus; LIO, left inferior occipital; LMTG, left middle temporal gyrus; LPF, left posterior frontal; LPT, left posterior temporal; post, posterior; M, male; RAH, right anterior hippocampus; RAM, right amygdala; RMO, right mesial occipital; RMTG, right middle temporal gyrus; RAM, right amygdala; RMF, right middle frontal; RPF, right posterior frontal; RPH, right posterior hippocampus; RPT, right posterior temporal; RSO, right superior occipital; RSTG, right superior temporal gyrus; RTFP, right temporal frontal parietal; and SAH, selective amygdalohippocampectomy.

Each patient underwent extensive clinical workup in our Comprehensive Epilepsy Program leading to their intracranial monitoring. EEG was recorded using depth macroelectrodes, subdural grids/strip, or a combination of electrode configurations. Specific use of electrode types and their locations are summarized in Table 1.

The patients studied were diverse and included those with both unilateral and bilateral seizure foci. Three patients had a clear right-sided seizure focus (patients 2, 5, and 6), two had a clear left-sided focus (patients 1 and 7), and two had ictal onset zones in either hemisphere (patients 3 and 4). All seizures but one (patient 7, seizure type 2) originated from the temporal lobe.

All patients ultimately underwent surgical resection of the putative seizure focus. Four patients had mild gliosis on pathological examination of resected tissue with MRI showing either no abnormalities (patients 4 and 6) or hippocampal atrophy (patients 5 and 7). Two patients had a pathological diagnosis of hippocampal sclerosis (patients 1 and 2), and one patient had a dysembryoplastic neuroepithelial tumor (patient 3). All except one of the patients became seizure-free postsurgery at the date of last follow-up (8–16 months follow-up).

Spatial localization of HFOs

Fast-sampling EEG (at 5 kHz) adequately captured HFOs that were evident on conventional review of the EEG recording (Figs. 1, A and B). HFOs were identified in all recordings from each patient, regardless of electrode type (Fig. 1A, strip electrode, and Fig. 2A, depth electrode). We used time-frequency analysis to explore two aspects of HFOs: (1) Spatial aspects pertaining to the location of HFOs relative to the ictal onset zone (based on conventional review of the EEG) and (2) temporal evolution of HFOs during the transition into seizures.

Fig. 1B shows the time frequency representation for the seizure shown in Fig. 1A. HFOs with a dominant frequency component of approximately 120 Hz were apparent starting 1 s prior to seizure onset and during the first several seconds of the seizure, after which slower spiking activity later predominated (0–40 Hz; Fig. 1B). The spatial analysis of HFO changes showed that the greatest increase in ictal HFO power was in the region of primary electrographic seizure onset (Fig. 1C).

The spatial distribution of HFOs was variable between patients, as shown in Fig. 3A. Despite this, the greatest ictal increase (positive *R*-value) in HFO power, specifically in the ripple and FR1 bands, was seen in the ictal onset channel(s) for all patients. In general, HFOs were localized to a single electrode in patients with well-defined seizure foci (patients 1 and 4). In patient 6, however, seizures originated from a single electrode but rapidly spread to neighboring contacts within the 5-s time span of analysis (i.e., 5 s ictal compared with 5 s preictal). Patients who had more broad lesions and/or broad seizure onset zones had HFOs with similar power over several contacts (i.e., patients 2 and 3). It should be noted that although power increases at the seizure focus were observed for all frequency bands, the greatest relative increases were seen in the ripple to FR3 bands (100–500 Hz).

Preictal elevations in HFO power amplitude manifest themselves as negative *R*-values and were also seen in some cases, such as patient 7 (left-sided seizure). Another patient with interesting HFO changes was patient 4 who exhibited independent seizures from the left and right hippocampus. This patient's typical clinical seizures were felt to be originating from the left hippocampus based on review of the VEM data. His right-sided seizures were felt to be of lesser clinical importance. He underwent a left selective amygdalohippocampectomy and is now seizure-free (7 months follow-up). Intriguingly, during right-sided seizures, the contacts that exhibited the greatest preictal change (negative *R*-values) corresponded to the electrode where the left-sided seizures originated. It is important to note that not all patients showed preictal HFO power increases. This may have occurred because ictal HFO power increases in some cases may have greatly exceeded preictal increases, resulting in positive *R*-values regardless of any preictal HFO power increases.

Fig. 3B shows the pooled results comparing HFO power for each frequency band for three contact locations: Seizure onset zone, an adjacent electrode, and a distant uninvolved electrode. Significant differences were observed only for ripple (100–200 Hz, $p < 0.05$) and a fast ripple band (300–400 Hz, $p < 0.005$) only when the seizure onset region was compared to a distant one (Fig. 3B). The low frequency band did not achieve statistical significance in any of the comparison permutations. These findings suggest that for the immediate preictal epoch, localized changes occur only for ripple and FR bands and only in the region of seizure onset.

Temporal HFO changes

Temporal analysis was performed for 30 min of EEG recording preceding the electrographic seizure onset. All data segments processed were free of artifact. No significant, reliable, or repeatable increases in HFO power were observed until approximately 30 s prior to electrographic seizure onset. We therefore considered this latter epoch for subsequent statistical analysis. We observed increases in HFO power amplitude and low frequency band (0–100 Hz) power starting 5 to 10 s prior to seizure onset (Fig. 4A). However, the sharpest increases were typically seen for HFO bands (100–500 Hz, Fig. 4A).

Fig. 4B shows the pooled results and statistical comparisons for temporal analysis for all patients for the origin, adjacent, and distant contacts. All HFO bands (100–500 Hz) in the origin and adjacent channels showed preictal

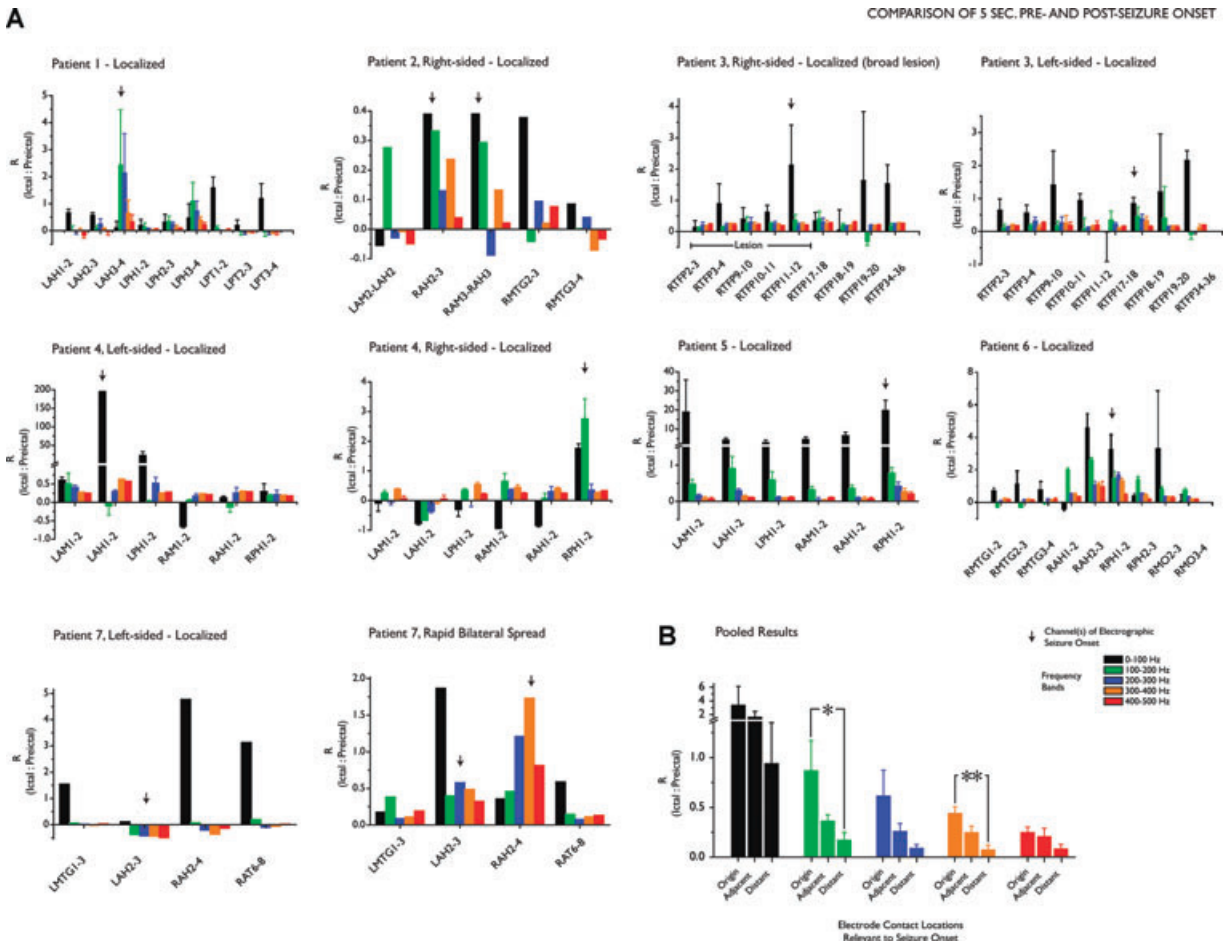

Figure 3.
Spatial distribution of HFOs in the preictal and early ictal periods for all patients. (**A**) Relative power ratio for each patient for each channel. When more than one seizure focus was seen in a patient, the seizures were grouped and analyzed separately. The greatest increase in *R*-values was typically observed in the channel(s) of ictal onset. Arrows mark channel of seizure onset as identified by expert visual review of the EEG. (**B**) Pooled data for all patients for all 20 seizures captured in all patients studied (see Table 1 for more details). *R*-values (mean ± sem) were compared using an ANOVA for each channel location across bands, and Student's *t*-tests were performed between permutations of channel locations within each band. Significant differences were observed for the 100–200 and 300–400 Hz bands. Statistical significance are denoted by *, $p < 0.05$; **, $p < 0.005$.

increases in power, whereas the power in the 0–100 Hz band increased later (Fig. 4B, left and center column). This marked difference can be better appreciated by looking at the raw magnitudes of the *R*-values for the distant channel, which were close to an order of magnitude smaller than those observed at the onset and adjacent channels. Time points that achieved statistical significance were found in the 100–200 Hz band beginning approximately 8 s prior to electrgraphic seizure onset and only when the origin channels were compared to a distant contact (Fig. 4B, $p < 0.05$). The low frequency band (0–100 Hz) power changes did not achieve statistical difference.

Discussion

In this study, we tested the feasibility of recording HFOs (ranging from 100–500 Hz) using commercially available depth and subdural grid electrodes using fast sampling EEG. In addition, we investigated the spatial and temporal attributes of HFOs with special consideration to the transition from preictal to ictal activity. Our study is the first to demonstrate that HFOs can reliably be recorded using commercially available intracranial depth electrodes. We also show that seizure onset is characterized by focal increases in HFOs that are localized to the ictal onset zone,

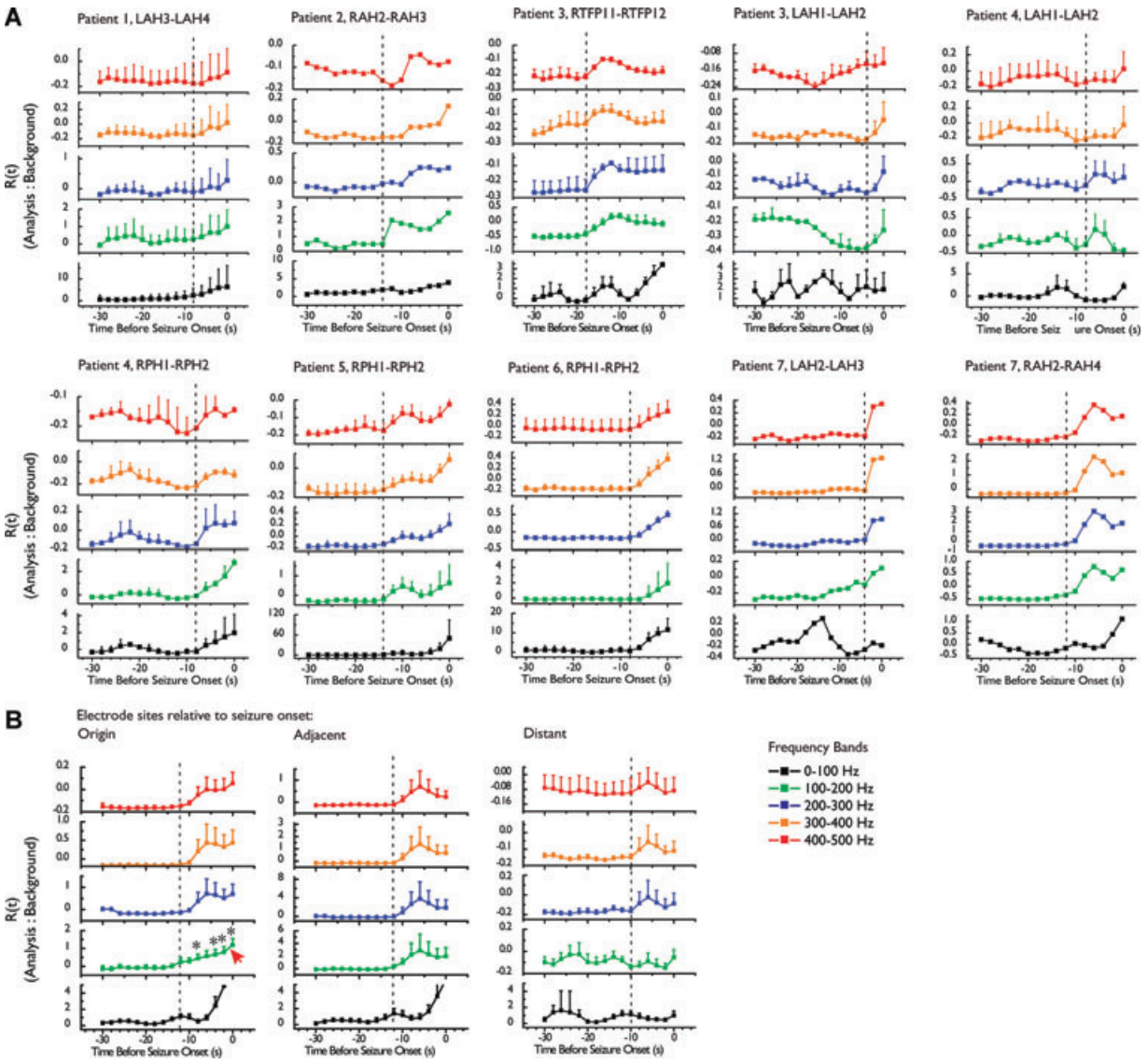

Figure 4.

Temporal trends in HFO power in the preictal period for all patients. (**A**) The relative power ratio changes over time [$R_{(f,c)}(t)$] for the ictal onset channels for 30 s leading up to seizure onset (mean ± SEM). In each case, the power amplitudes for all bands increased just prior to seizure onset (vertical dashed line). However, the HFO bands (>100 Hz) repeatedly exhibited a sharp and consistent increase during that epoch, which often preceded low frequency changes (e.g., see patients 2; 3, grid electrodes RTFP11-RTFP12; and 5). (**B**) Pooled data for relative power ratio changes over time (mean ± SEM) for all patients, for each band, for the three different channels: Ictal onset channel, immediately adjacent channel, and a distant uninvolved channel. Significant changes were seen for the 100–200 Hz band for approximately 8 s prior to seizure onset, when compared to a distant contact (**B**, red arrowhead, $p < 0.05$).

which is consistent with recent findings by other groups (Jirsch et al., 2006; Ochi et al., 2007; Urrestarazu et al., 2007). Furthermore, we observed that focal electrographic seizures were associated with better localized HFO changes compared to seizures with more broad seizure onset zones. We also observed that HFO power amplitudes exhibit a gradual increase, beginning about 8 s prior to seizure onset. It is important to note that both the spatial and temporal changes observed were most significant for HFO frequency bands and not low frequencies. This suggests that HFOs can act as markers of epileptogenic neuronal network activity.

It is also important to consider the contribution and trends observed for lower frequency oscillations (0–100 Hz), since they also increased in absolute magnitude in many cases. This increase was observed in either the channel of primary seizure onset (e.g., patient 4, left-sided seizure) and at times in neighboring channels (e.g., patient 6). Indeed, the *R*-values for the 0–100 Hz band, in both spatial and temporal analysis, are larger in many instances than any of the HFO-associated bands (i.e., 100–500 Hz). This observation can be attributed to a combination of physiological and analysis-related parameters, respectively. One known effect that would preferentially bias 0–100 Hz *R*-values towards larger numbers is the well-described intrinsic *1/f* frequency scaling relation observed in power spectral density of EEG signals, where power spectral amplitudes are inversely related to frequency (Freeman et al., 2006). The precise reason for this *1/f* frequency scaling remains unknown, but it is believed to reflect an aspect of neuronal network dynamics (Bédard et al., 2006). Nonetheless, the fact that power increases were seen in both low frequency and HFO bands suggests that these signal components may be linked as they reflect underlying network dynamics. Also, HFOs are typically of low amplitude and override larger slower frequency waveforms that may predominate the early phases of an electrographic seizure.

HFO recordings with commercial electrodes

Our observation that HFOs can be recorded using commercially available depth electrodes (effective area, 7.2 mm^2) is an extension of recent studies in which HFOs were recorded using custom-built depth macroelectrodes with a smaller effective area of 0.8–0.85 mm^2 (Jirsch et al., 2006; Urrestarazu et al., 2006). In addition, our work is consistent with previous observations that HFOs in the 100–200 Hz band can be recorded using commercially available grid electrodes (Akiyama et al., 2005, 2006; Ochi et al., 2007). Taken together, our study, along with previous reports, suggests that HFO generators may be comprised of larger clusters of neurons than previously believed. Nonetheless, it is acknowledged that microelectrode recordings still have specific advantages over macroelectrode recordings, including greater sensitivity in detecting HFOs due to their fine spatial sampling (Bragin et al., 1999a, 1999b, 2003; Chrobak & Buzsaki, 1994).

Spatial localization of HFOs

We showed that the HFOs with the greatest amplitudes were localized to the channel(s) of ictal onset. Moreover, the number of involved electrode contacts was proportional to the size of the seizure onset zone. For example, patients with focal unilateral seizures (e.g., patients 1 and 4) showed a more localized area of HFO changes compared to those patients with more diffuse brain abnormalities (e.g., patient 3; Fig. 3). In addition, when the total *R*-values were summed for >100 Hz for each channel in each patient, the totals were consistently the greatest for all ictal onset channels, although this trend did not achieve statistical significance. It is possible that these trends may have achieved statistic significance if more patients were able to be included in this study. Our observations are consistent with those of Jirsch et al. (2006) who did not observe significant HFO content in the EEG of patients with poor seizure localization. Therefore, our findings suggest that HFOs may be generated by local, pathologically altered clusters of neurons that may play a role in generating seizures and that HFOs may be direct markers of seizure-generating networks (Bragin et al., 2004).

The localized nature of HFO changes suggests that their presence may be a useful clinical tool in the demarcation of onset zones for tailored surgical resections. Indeed, in our small series, all patients were seizure-free following resection, except patient 7. This patient was unique in that HFOs were of greatest magnitude in the side opposite to surgical resection (Fig. 3A). Thus, HFO analysis may also be useful in identifying the side of greater seizure susceptibility. In addition, localization of HFOs may be useful for predicting outcome after surgery in patients with extratemporal epilepsy (Ochi et al., 2007). Further, prospective studies with longer follow-up periods are needed to properly assess the utility of HFOs in this capacity.

Temporal HFO changes and the preictal state

We have shown that HFO power undergoes a measurable and robust increase in the immediate preictal epoch that is localized to the ictal onset zone. These changes may be indicative of preictal changes in the states of activity in localized neuronal networks and possibly larger brain beyond the ictal onset zone. The cellular and network parameters that govern HFO dynamics in the preictal period remain unclear. Nonetheless, it is possible to speculate on potential mechanisms. Studies of in vitro seizure models suggest that seizure precursors may begin locally as a series of rhythmic discharges. As the discharges become more frequent, adjacent or distant projection sites become recruited, thereby heralding oncoming seizures (Dzhala & Staley, 2003). Moreover, it has been suggested that neuronal synchrony changes in the transition into seizures (Garcia Dominguez et al., 2005).

There is evidence that HFOs can be caused by alterations in excitatory, inhibitory, and gap-junctional communication (reviewed by Rampp & Stefan, 2006). It is important to note that individual cell firing rates do not approach the full range of FR activity (i.e., >300 Hz) in either in vitro seizure models (Lasztoczi et al., 2004) or in unit recordings in patients (Isokawa-Akesson et al., 1987). Therefore, it has been postulated that field oscillatory rhythms, such as ripples and FRs, arise from population activity from neurons that have variable firing rates and phases (Brunel & Wang, 2003; Geisler et al., 2005). In other words, HFOs represent rapid changes in phase within

an overall synchronous state that defines seizure activity. It has also been suggested that formation of ripple, and presumably FR population activity, depends strongly on single-cell membrane dynamics that are modulated by inhibitory and excitatory inputs (Geisler et al., 2005). In particular, the synchrony of inhibitory cells seems to be a required parameter for the generation of faster field oscillations. Thus, preictal HFO power increases may reflect rapid changes in local network synchrony that are modulated by inhibitory networks, which themselves have undergone modifications in the epileptic brain (Cossart et al., 2005).

It may be argued that the short period (seconds) prior to seizure onset in which HFO power increases are first seen may be considered ictal onset rather than a preictal period. This is a valid concern that we believe is a matter of definition that also reflects the novelty of a preictal state and preictal HFO changes. Indeed, it is very challenging to identify a precise electrographic onset that is a truly objective on the order of a few seconds. Ideally, preictal EEG changes should be measurable on the order of minutes to hours. However, no study to date has shown reliable preictal EEG changes in this time frame despite using various computational techniques (Mormann et al., 2007). On the other hand, a number of other physiological measures or clinical phenomena are known to change in the minutes or hour leading up to seizure onset, including functional MRI signals (Federico et al., 2005), cerebral blood flow (Weinand et al., 1997; Baumgartner et al., 1998), and heart rate (Delamont et al., 1999; Leutmezer et al., 2003). Thus, a preictal physiological state exists, and it may represent a fundamental process in the initiation of seizures. Furthermore, one of the last identifiable changes in the preictal period may be increased HFO power, which in turn, may increase neuronal synchronization.

Conclusions and future work

We have shown that HFOs can be recorded using commercially available depth and grid electrodes in patients with temporal lobe epilepsy. In addition, the spatial localization of HFOs varies with the spatial extent of the ictal onset zone. HFOs appeared to colocalize with the critical ictal onset zone. Indeed, all patients who had resection of tissue exhibiting HFOs are currently seizure-free, whereas the one patient who did not is currently experiencing seizures. HFOs also undergo robust increases in power in the immediate preictal period. Overall, our findings suggest that HFOs may be markers of neuronal network activity that represent a fundamental precursor to seizure initiation.

Understanding how, where, and why preictal HFO and other physiological changes occur is of interest for several reasons. At present, HFOs appear to be good markers for localizing the ictal onset zone and thereby possess the potential of enhancing the delivery of current treatments such as surgical resection. Another reason to study HFOs is that they can be used, perhaps with other EEG quantifiers, to possibly anticipate seizure onset, which at present remains a challenging problem (Litt & Krieger, 2007; Mormann et al., 2007). This, in turn, may help guide the location and timing of future therapeutic interventions such as on-demand deep brain stimulation or direct drug delivery devices. Finally, a better understanding of mechanisms underlying the interictal-to-ictal transition may unmask fundamental mechanisms that may help develop novel therapeutic strategies.

Acknowledgments

We are grateful to the patients for their participation. We are thankful for assistance of the EEG technologists at the Foothills Medical Centre, with special thanks to Susan Campbell, Lindsay Oliverio, and Erin Phillip. H.K. is supported by MD/PhD studentships from Canadian Institutes for Health Research (CIHR) and Alberta Heritage Foundation for Medical Research (AHFMR). This work was supported by operating grants awarded to P.F. from the American Epilepsy Society, CIHR, and AHFMR.

Conflict of interest: We confirm that we have read the Journal's position on issues involved in ethical publication and affirm that this report is consistent with those guidelines. None of the authors have any conflicts of interest to disclose.

References

Akiyama T, Otsubo H, Ochi A, Ishiguro T, Kadokura G, Ramachandrannair R, Weiss SK, Rutka JT, Carter Snead O 3rd. (2005) Focal cortical high-frequency oscillations trigger epileptic spasms: confirmation by digital video subdural EEG. *Clin Neurophysiol* 116:2819–2825.

Akiyama T, Otsubo H, Ochi A, Galicia EZ, Weiss SK, Donner EJ, Rutka JT, Snead OC 3rd. (2006) Topographic movie of ictal high-frequency oscillations on the brain surface using subdural EEG in neocortical epilepsy. *Epilepsia* 47:1953–1957.

Baumgartner C, Serles W, Leutmezer F, Pataraia E, Aull S, Czech T, Pietrzyk U, Relic A, Podreka I. (1998) Preictal SPECT in temporal lobe epilepsy: regional cerebral blood flow is increased prior to electroencephalography-seizure onset. *J Nucl Med* 39:978–982.

Bédard C, Kröger H, Destexhe A. (2006) Does the 1/f frequency scaling of brain signals reflect self-organized critical states? *Phys Rev Lett* 97:118102.

Bragin A, Engel J Jr, Wilson CL, Fried I, Buzsaki G. (1999a) High-frequency oscillations in human brain. *Hippocampus* 9:137–142.

Bragin A, Engel J Jr, Wilson CL, Fried I, Mathern GW. (1999b) Hippocampal and entorhinal cortex high-frequency oscillations (100–500 Hz) in human epileptic brain and in kainic acid–treated rats with chronic seizures. *Epilepsia* 40:127–137.

Bragin A, Engel J Jr, Wilson CL, Vizentin E, Mathern GW. (1999c) Electrophysiologic analysis of a chronic seizure model after unilateral hippocampal KA injection. *Epilepsia* 40:1210–1221.

Bragin A, Mody I, Wilson CL, Engel J Jr. (2002a) Local generation of fast ripples in epileptic brain. *J Neurosci* 22:2012.

Bragin A, Wilson CL, Staba RJ, Reddick M, Fried I, Engel J Jr. (2002b) Interictal high-frequency oscillations (80–500 Hz) in the human epileptic brain: entorhinal cortex. *Ann Neurol* 52:407.

Bragin A, Wilson CL, Engel J. (2003) Spatial stability over time of brain areas generating fast ripples in the epileptic rat. *Epilepsia* 44:1233–1237.

Bragin A, Wilson CL, Almajano J, Mody I, Engel J Jr. (2004) High-frequency oscillations after status epilepticus: epileptogenesis and seizure genesis. *Epilepsia* 45:1017–1023.

Brunel N, Wang XJ. (2003) What determines the frequency of fast network oscillations with irregular neural discharges? I. Synaptic

dynamics and excitation-inhibition balance. *J Neurophysiol* 90: 415–430.

Buzsaki G, Horvath Z, Urioste R, Hetke J, Wise K. (1992) High-frequency network oscillation in the hippocampus. *Science* 256:1025–1027.

Chrobak JJ, Buzsaki G. (1994) Selective activation of deep layer (V-VI) retrohippocampal cortical neurons during hippocampal sharp waves in the behaving rat. *J Neurosci* 14:6160–6170.

Cossart R, Bernard C, Ben-Ari Y. (2005) Multiple facets of GABAergic neurons and synapses: multiple fates of GABA signalling in epilepsies. *Trends Neurosci* 28:108–115.

Curio G, Mackert BM, Burghoff M, Koetitz R, Abraham-Fuchs K, Harer W. (1994) Localization of evoked neuromagnetic 600 Hz activity in the cerebral somatosensory system. *Electroencephalogr Clin Neurophysiol* 91:483–487.

Curio G. (2000) Linking 600-Hz ''spikelike'' EEG/MEG wavelets (''sigma-bursts'') to cellular substrates: concepts and caveats. *J Clin Neurophysiol* 17:377–396.

Delamont RS, Julu PO, Jamal GA. (1999) Changes in a measure of cardiac vagal activity before and after epileptic seizures. *Epilepsy Res* 35:87–94.

Draguhn A, Traub RD, Bibbig A, Schmitz D. (2000) Ripple (approximately 200-Hz) oscillations in temporal structures. *J Clin Neurophysiol* 17:361–376.

Dzhala VI, Staley KJ. (2003) Transition from interictal to ictal activity in limbic networks in vitro. *J Neurosci* 23:7873–7880.

Federico P, Abbott DF, Briellmann RS, Harvey AS, Jackson GD. (2005) Functional MRI of the pre-ictal state. *Brain* 128:1811–1817.

Fisher RS, Webber WR, Lesser RP, Arroyo S, Uematsu S. (1992) High-frequency EEG activity at the start of seizures. *J Clin Neurophysiol* 9:441–448.

Freeman WJ, Holmes MD, West GA, Vanhatalo S. (2006) Fine spatiotemporal structure of phase in human intracranial EEG. *Clin Neurophysiol* 117:1228–1243.

Garcia Dominguez L, Wennberg RA, Gaetz W, Cheyne D, Snead OC 3rd, Perez Velazquez JL. (2005) Enhanced synchrony in epileptiform activity? Local versus distant phase synchronization in generalized seizures. *J Neurosci* 25:8077–8084.

Geisler C, Brunel N, Wang XJ. (2005) Contributions of intrinsic membrane dynamics to fast network oscillations with irregular neuronal discharges. *J Neurophysiol* 94:4344–4361.

Isokawa-Akesson M, Wilson CL, Babb TL. (1987) Diversity in periodic pattern of firing in human hippocampal neurons. *Exp Neurol* 98: 137–151.

Jirsch JD, Urrestarazu E, LeVan P, Olivier A, Dubeau F, Gotman J. (2006) High-frequency oscillations during human focal seizures. *Brain* 129:1593–1608.

Khosravani H, Pinnegar CR, Mitchell JR, Bardakjian BL, Federico P, Carlen PL. (2005) Increased high-frequency oscillations precede in vitro low-Mg seizures. *Epilepsia* 46:1188–1197.

Lasztoczi B, Antal K, Nyikos L, Emri Z, Kardos J. (2004) High-frequency synaptic input contributes to seizure initiation in the low-[Mg^{2+}] model of epilepsy. *Eur J Neurosci* 19:1361–1372.

Leutmezer F, Schernthaner C, Lurger S, Potzelberger K, Baumgartner C. (2003) Electrocardiographic changes at the onset of epileptic seizures. *Epilepsia* 44:348–354.

Litt B, Lehnertz K. (2002) Seizure prediction and the preseizure period. *Curr Opin Neurol* 15:173–177.

Litt B, Krieger A. (2007) Of seizure prediction, statistics, and dogs: a cautionary tail. *Neurology* 68:250–251.

Mormann F, Andrzejak RG, Elger CE, Lehnertz K. (2007) Seizure prediction: the long and winding road. *Brain* 130:314–333.

Ochi A, Otsubo H, Donner EJ, Elliott I, Iwata R, Funaki T, Akizuki Y, Akiyama T, Imai K, Rutka JT, Snead OC 3rd. (2007) Dynamic changes of ictal high-frequency oscillations in neocortical epilepsy: using multiple band frequency analysis. *Epilepsia* 48:286–296.

Rampp S, Stefan H. (2006) Fast activity as a surrogate marker of epileptic network function? *Clin Neurophysiol* 117:2111–2117.

Siapas AG, Wilson MA. (1998) Coordinated interactions between hippocampal ripples and cortical spindles during slow-wave sleep. *Neuron* 21:1123–1128.

Staba RJ, Wilson CL, Bragin A, Fried I, Engel J Jr. (2002) Quantitative analysis of high-frequency oscillations (80–500 Hz) recorded in human epileptic hippocampus and entorhinal cortex. *J Neurophysiol* 88:1743–1752.

Staba RJ, Wilson CL, Bragin A, Jhung D, Fried I, Engel J Jr. (2004) High-frequency oscillations recorded in human medial temporal lobe during sleep. *Ann Neurol* 56:108–115.

Staba RJ, Frighetto L, Behnke EJ, Mathern GW, Fields T, Bragin A, Ogren J, Fried I, Wilson CL, Engel J Jr. (2007) Increased fast ripple to ripple ratios correlate with reduced hippocampal volumes and neuron loss in temporal lobe epilepsy patients. *Epilepsia* 48:2130–2138.

Traub RD, Whittington MA, Buhl EH, LeBeau FE, Bibbig A, Boyd S, Cross H, Baldeweg T. (2001) A possible role for gap junctions in generation of very fast EEG oscillations preceding the onset of, and perhaps initiating, seizures. *Epilepsia* 42:153–170.

Traub RD, Draguhn A, Whittington MA, Baldeweg T, Bibbig A, Buhl EH, Schmitz D. (2002) Axonal gap junctions between principal neurons: a novel source of network oscillations, and perhaps epileptogenesis. *Rev Neurosci* 13:1–30.

Urrestarazu E, Jirsch JD, LeVan P, Hall J, Avoli M, Dubeau F, Gotman J. (2006) High-frequency intracerebral EEG activity (100–500 Hz) following interictal spikes. *Epilepsia* 47:1465–1476.

Urrestarazu E, Chander R, Dubeau F, Gotman J. (2007) Interictal high-frequency oscillations (100–500 Hz) in the intracerebral EEG of epileptic patients. *Brain* 130:2354–2366.

Weinand ME, Carter LP, el-Saadany WF, Sioutos PJ, Labiner DM, Oommen KJ. (1997) Cerebral blood flow and temporal lobe epileptogenicity. *J Neurosurg* 86:226–232.